Inhibition of ornithine decarboxylase alters the roscovitine-induced mitochondrial-mediated apoptosis in MCF-7 breast cancer cells

ELIF DAMLA ARISAN, PINAR OBAKAN, AJDA COKER and NARCIN PALAVAN-UNSAL

Department of Molecular Biology and Genetics, Faculty of Science and Letters, Istanbul Kultur University, Istanbul, Turkey

Abstract. Polyamines (PAs) are small aliphatic amines that play a major role in multicellular functions. The PA levels are controlled by ornithine decarboxylase (ODC), the rate limiting enzyme of PA biosynthesis. α-difluoromethylornithine (DFMO) is the ODC inhibitor, which has been shown to act as an antiproliferative agent in human cancer cells by irreversibly inhibiting ODC, which is overexpressed in breast cancer cells. Roscovitine (ROSC; CYC202), a selective cyclin-dependent kinase inhibitor, induces cell cycle arrest and concomitantly apoptosis in tumor cells. In this study, we aimed to investigate the possible role of PAs in ROSC-induced apoptosis in estrogen-dependent MCF-7 breast cancer cells. Cell viability was assessed following the exposure of MCF-7 cells to DFMO and/or ROSC by MTT cell viability assay. To evaluate the drug-induced apoptotic events, DNA fragmentation by Cell Death ELISA assay and 4,6-diamidino-2-phenylindole staining, were utilized. The disruption of mitochondrial membrane potential, caspase-9 and PARP cleavage was also determined in order to investigate the role of mitochondrial-mediated apoptosis. The modulation of Bcl-2 family members was also evaluated using the immunoblotting technique. Drug-induced reactive oxygen species was determined by a fluorometer following 2',7'-dichlorofluorescein diacetate staining. We found that ROSC induced apoptosis in a dose- and caspase-dependent manner. The ODC specific inhibitor, DFMO, altered the apoptotic effects of ROSC by increasing the generation of reactive oxygen species, decreasing the PA intracellular pool and modulating pro-apoptotic and anti-apoptotic Bcl-2 family members. All these findings suggest that ODC may be a critical target for evaluating the PA metabolic pathway as a therapeutic target in ROSC-induced mitochondrial-mediated apoptotis in estrogen-dependent MCF-7 breast cancer cells.

Introduction

Breast cancer is the most diagnosed type of cancer in women and the second leading cause of cancer-related mortality worldwide (1). Despite the presence of new promising advances in therapeutics, the breast cancer mortality rate is increasing. Current treatments for this malignancy are generally focused on reducing estrogen levels, which promote disease progression. However, breast cancer cells escape from the estrogen ablation therapy due to their ability to grow estrogen-independently (2). The successful treatment regime for these aggressive and fast growing tumors remains unclear.

New therapeutic approaches for breast cancer prevention, such as targeting the cell cycle regulatory mechanism, are still being investigated. The inhibition of cyclin-dependent kinases (CDKs) that are involved in the regulation of the cell cycle is an attractive therapeutic strategy. Roscovitine (ROSC) is a small purine-like CDK inhibitor which has increased selectivity towards CDK1, CDK2, CDK7 and CDK9 (3-5). Previous studies have shown that ROSC treatment causes cell cycle arrest in various cancer types, and *in vitro* studies have revealed that ROSC significantly induces cell cycle arrest in estrogen-dependent MCF-7 breast cancer cells (6).

The polyamines (PAs), putrescine (Put), spermidine (Spd) and spermine (Spm), are amine-derived cationic molecules, which play crucial roles in the regulation of the cell cycle. The activation of the PA biosynthetic pathway also leads to the accumulation of intracellular PAs, which are critical in disease progression. In addition, intracellular PA content has also been shown to be higher in breast tumors than normal breast tissue (7,8).

The PA rate-limiting biosynthetic enzyme, ornithine decarboxylase (ODC), is responsible for PA accumulation and has been shown to be upregulated in breast cancer cells (9-11).

Correspondence to: Dr Elif Damla Arisan, Department of Molecular Biology and Genetics, Faculty of Science and Letters, Istanbul Kultur University, Atakoy Campus, 34156 Istanbul, Turkey
E-mail: d.arisan@iku.edu.tr

Abbreviations: CDKs, cyclin-dependent kinases; DCFH-DA, 2',7'-dichlorofluorescein diacetate; DiOC$_6$(3), 3,3'-dihexyloxacarbocyanine iodide; DFMO, α-difluoromethylornithine; DMEM, Dulbecco's modified Eagle's medium; DMSO, dimethyl sulfoxide; HPLC, high pressure liquid chromatography; ODC, ornithine decarboxylase; PA, polyamine; PAO-N^1, polyamine oxidase; PBS, phosphate-buffered saline; Put, putrescine; PVDF, polyvinylidene difluoride; ROSC, roscovitine; SDS, sodium dodecyl sulphate; SMO/PAOh1, spermine oxidase; Spd, spermidine; Spm, spermine; SSAT, spermidine/ spermine N1-acetyltransferase; $\Delta_{\psi m}$, mitochondrial membrane potential

Key words: polyamines, α-difluoromethylornithine, ornithine decarboxylase, cyclin-dependent kinases inhibitor, roscovitine

Previous studies have shown that ODC may be involved in neoplastic transformation in cells by activating several proto-oncogenes, such as c-myc. Consequently, the utilization of specific inhibitors of PA biosynthesis has been indicated as a potential blocker of tumor progression (12).

The specific inhibitor, α-difluoromethylornithine (DFMO), is an irreversible inhibitor of ODC. It has been shown that DFMO acts as an antitumoral agent by decreasing Put and Spd levels, which causes cell cycle arrest in cells. DFMO also inhibits the metastatic potential in various cancer cells (13-16).

In this study, we aimed to evaluate the possible role of PAs in ROSC-induced apoptosis. Our results indicate that DFMO alters the ROSC-induced apoptosis by activating mitochondrial-mediated cell death in MCF-7 cells.

Materials and methods

Cell culture. MCF-7 breast cancer cells (HTB-22; ATCC, Middlesex, UK) were grown in Dulbecco's modified Eagle's medium (DMEM) (PAN Biotech, Aidenbach, Germany) medium supplemented with 4 mM L-glutamine and 3.7 g/l sodium carbonate, 10% fetal bovine serum (PAN Biotech) and penicillin-streptomycin (10,000 units penicillin/ml, 10 mg streptomycin/ml) at 37°C in a humidified 5% CO_2 incubator (Biological Industries, Kibbutz Beit-Haemek, Israel). Cells were seeded overnight and then treated with DFMO [(Sigma, St. Louis, MO, USA; 10 mM stock concentration in dimethyl sulfoxide (DMSO)] and/or ROSC (Calbiochem, San Diego, CA, USA; 10 mM stock concentration in DMSO) and stored at -20°C.

Determination of cell viability. MCF-7 breast cancer cells were seeded at a $1x10^4$ density per well in 96-well plates. Cells were exposed to various concentrations of DFMO or ROSC for 24 h at concentrations ranging from 0 to 5 mM and 0 to 100 μM, respectively. Ten microliters 3-(4,5-dimethylthiazol-2-yl)-2,5- diphenyl tetrazolium bromide dye (5 mg/ml; Sigma) were added to each well and cells were kept at 37°C for 4 h. The resulting formazan crystals were solubilized in 200 μl DMSO (Sigma). The density of the resolubilized formazan product was read at 570 nm spectrophotometrically (Bio-Rad, Hercules, CA, USA).

Detection of apoptotic cells with 4,6-diamidino-2-phenylindole (DAPI) staining. For visualization of nuclei, cells were stained with DAPI dissolved in phosphate-buffered saline (PBS) at a final concentration of 1 μg/ml (Molecular Probes, Eugene, OR, USA). Cells were visualized with fluorescent microscopy (Olympus, Japan).

Detection of mitochondrial membrane potential ($\Delta_{\psi m}$) disruption. MCF-7 cells ($1x10^5$) were seeded in 12-well plates. Following exposure of cells to the drugs, they were washed once with PBS, and then stained with a 4 nM 3,3'-dihexyloxa-carbocyanine iodide [$DiOC_6(3)$] (Calbiochem, La Jolla, CA, USA; 40 nM stock concentration in DMSO) fluorescent probe. $\Delta_{\psi m}$ disruption was visualized under a fluorescence micro-scope (Olympus) (excitation/emission = 488/525 nm).

Quantification of DNA fragmentation. Apoptosis was deter-mined with the Cell Death ELISA Plus kit (Roche, Indianapolis,

IN, USA). Briefly, $1x10^4$ MCF-7 cells were seeded into 96-well plates and then treated with DFMO and/or ROSC for 24 h. They were harvested and lysed according to the manufacturer's instructions. The samples were transferred into 96-well plate dishes coated with a mouse monoclonal antibody against histone complexes. After incubation and washing steps, anti-DNA-peroxidase was added into the wells. The reaction was developed with the substrate supplied by the manufacturer and the absorbance read at 410 nm (Bio-Rad).

Colorimetric caspase-6 activity assay. Caspase-6 activity was measured using the ApoTarget assay (Invitrogen, San Diego, CA, USA), as recommended by the manufacturer. The activity was normalized according to total protein content curve, which was obtained from the Bradford assay.

Determination of ROSC-induced caspase-dependent apop-tosis. Both negative caspase inhibitor (Z-FA-FMK) and caspase-9 inhibitor (Z-LEHD-FMK) (BD Biosciences, San Jose, CA, USA; each 20 μM) were used to evaluate the potential roles of caspase-9 in ROSC-induced apoptosis in the presence or absence of DFMO. Inhibitors were stored at -20°C as a 100 mM stock solution in DMSO. Cells were incubated with inhibitors for 2 h prior to treatment with ROSC and/or DFMO.

Western blot analysis. MCF-7 cells were lysed in ProteoJET Mammalian cell lysis reagent (Fermantas, Hanover, MD, USA) containing total protease inhibitor cocktail. Total cellular protein levels were determined by the Bradford method (Bio-Rad). To proceed with immunoblotting, 20 μg of total protein was loaded onto 10% sodium dodecyl sulphate (SDS)-polyacrylamide gels and subjected to electrophoresis. Gels were electrophoretically transferred to polyvinylidene difluoride (PVDF) membranes (Roche). PVDF membranes were rinsed in tris-buffered saline with Tween-20 (TBS-T) [10 mM Tris-HCl (pH 8), 0.05% Tween-20] and blocked in a buffer of TBS-T containing 5% skim milk overnight at 4°C. PVDF membranes were then incubated with primary antibodies (Bcl-2, Bcl-x_L, Bax, Puma, Bad, caspase-9, PARP and β-actin; Cell Signaling Technology, Danvers, MA, USA) overnight at 4°C. Membranes were then incubated with secondary antibodies (anti-rabbit IgG), conjugated to horseradish peroxidase for 2 h at room temperature. Membranes were developed using ECL chemi-luminescence reagents (Amersham Pharmacia Biotech, Little Chalfont, UK) and exposed to X-ray films (Hyperfilm-ECL; Amersham Pharmacia Biotech). Densitometric analysis of immunoblots was performed using ImageJ 1.37v software; all proteins were quantified relative to the loading control.

Measurement of reactive oxygen species. In order to determine drug-induced reactive oxygen species generation 2',7'-dichloro-fluorescein diacetate (DCFH-DA; Calbiochem) was utilized for 30 min at 37°C. Results were obtained by fluorescence micros-copy (Olympus) at 485 nm excitation and 520 nm emission.

Measurement of PA levels. Cells ($3x10^5$) were harvested from 6-well culture Petri dishes, washed twice with PBS and pellet-ized. The cell pellet was treated with 50% tricholoroacetic acid and centrifuged at 13,200 rpm for 20 min. Supernatant was kept and benzoylation was performed. PA levels were

determined by high pressure liquid chromatography (HPLC) (Agilent Technologies, Palo Alto, CA, USA) as described by Singh *et al* (17).

Statistics. Results were obtained from the averages of at least two experiments and analyzed with Graph Pad 4.04 version software. Immunoblotting results were repeated at least twice and ImageJ program was applied to get band intensities. To determine significant alterations, a two-tailed unpaired t-test was performed.

Results

Inhibition of PA biosynthesis modulates ROSC-induced apoptosis in MCF-7 cells. Cell viability assay was determined following treatment with the drugs at various concentrations for 24 h in MCF-7 cells. As shown in Fig. 1A. ROSC decreased cell viability in a dose-dependent manner. According to the MTT cell viability assay, exposure of cells to 20 μM ROSC for 24 h had moderate cytotoxic effects (20% decrease in cell viability vs. control; p=0.0003). Although ROSC significantly decreased cell viability compared to the control samples, dose-dependent studies showed that DFMO did not exert any effect on MCF-7 cells (Fig. 1B). In addition, 20 μM ROSC was combined with a non-cytotoxic dose of DFMO (2.5 mM) and then cell viability assay was carried out. We found that co-treatment with DFMO and ROSC for 24 h decreased cell viability by 39.4% compared to the control samples (p=0.0004). Further studies were designed using these drug concentrations for ROSC and DFMO in MCF-7 cells to evaluate nuclear fragmentation, as well as apoptosis, as shown in Fig. 1B by fluorescent microscopy following DAPI staining.

In order to investigate the cell viability loss due to apoptotic induction, MCF-7 cells were exposed to ROSC (20 μM), DFMO (2.5 mM) or the combination of both for 24 h. As shown in Fig. 2A, ROSC significantly increased DNA fragmentation by ~10-fold compared to the control samples (p=0.0126). Although the specific ODC inhibitor did not exert any apoptotic stimulation (p=0.12 vs. control), it significantly increased the levels of DNA fragmentation following ROSC treatment by 1.5-fold (p=0.002). Furthermore, $\Delta_{\psi m}$ was decreased in response to the ROSC and DFMO combined treatment. ROSC (20 μM) caused significant decrease in $\Delta_{\psi m}$ by 59±0.7% (p<0.0001 vs. control). In the presence of DFMO (2.5 mM), ROSC further increased $\Delta_{\psi m}$ by 79.42±0.28% (Fig. 2B).

To evaluate the potential role of caspases in ROSC-induced apoptosis, we determined caspase-9 cleavage following ROSC treatment in the presence or absence of DFMO. We determined that ROSC treatment induced caspase-9 activity, and PA depletion increased the ROSC-induced pro-caspase-9 cleavage (Fig. 2C). In our experiments, the specific caspase-9 inhibitor, Z-LEHD-FMK, was used to address the significance of caspase activation. Cells were exposed to the caspase-9 inhibitor for 2 h, and were then treated with ROSC in the presence or absence of DFMO. Cytotoxicity was evaluated by MTT cell viability assay (Fig. 2D). Pre-treatment with the caspase-9 inhibitor (20 μM) prevented the cytotoxic effects of ROSC in the presence or absence of DFMO (p=0.02) compared to the control samples. In order to understand the potential role of caspase-6 as an executioner caspase in the downstream target
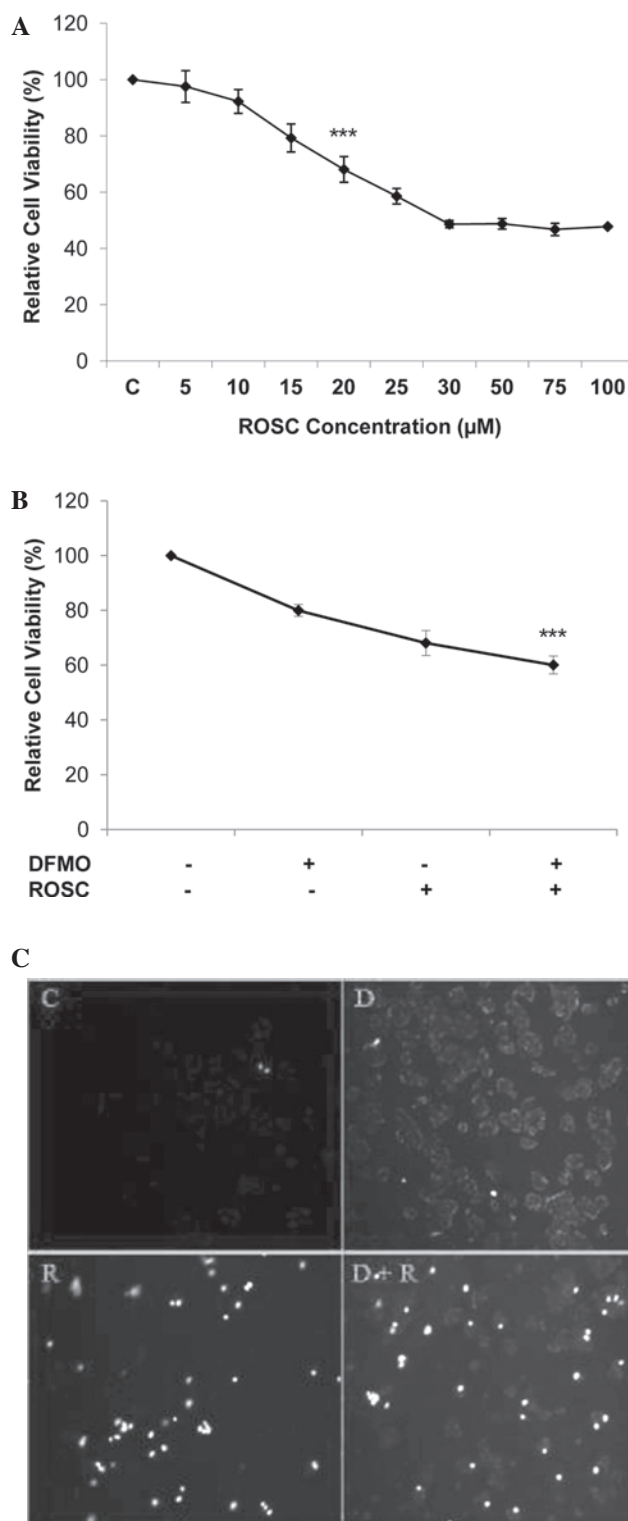
Figure 1. ROSC induced cell viability loss in a dose-dependent manner and co-treatment with DFMO enhanced the cytotoxic effects of ROSC in MCF-7 cells. (A) Cells (1x10^4) were seeded into a 96-well plate and treated with various concentrations of ROSC (0-50 μM) for 24 h. ROSC (20 μM) was combined with 2.5 mM DFMO and MTT assay was performed to detect the MCF-7 cell viability. Graphs represent the means ± SD of at least 3 experiments with 5 replicates. Statistical difference was analyzed using the Student's t-test; ***p=0.0002. (B) 20 μM of ROSC combined with 2.5 mM DFMO and MTT assay was performed to detect the MCF-7 cell viability. Graphs represent the mean ± SD of at least three experiments with five replicates. Statistical differences were analyzed according to the Student t-test. ***p=0.0004. (C) Cells (1x10^5) were seeded on 12-well plates and treated with ROSC, DFMO or with a combination for 24 h and DAPI staining was performed to detect the apoptotic cells. C, control, untreated cells; DFMO, α-difluoromethylornithine; ROSC, roscovitine.

A

B

C

D

E
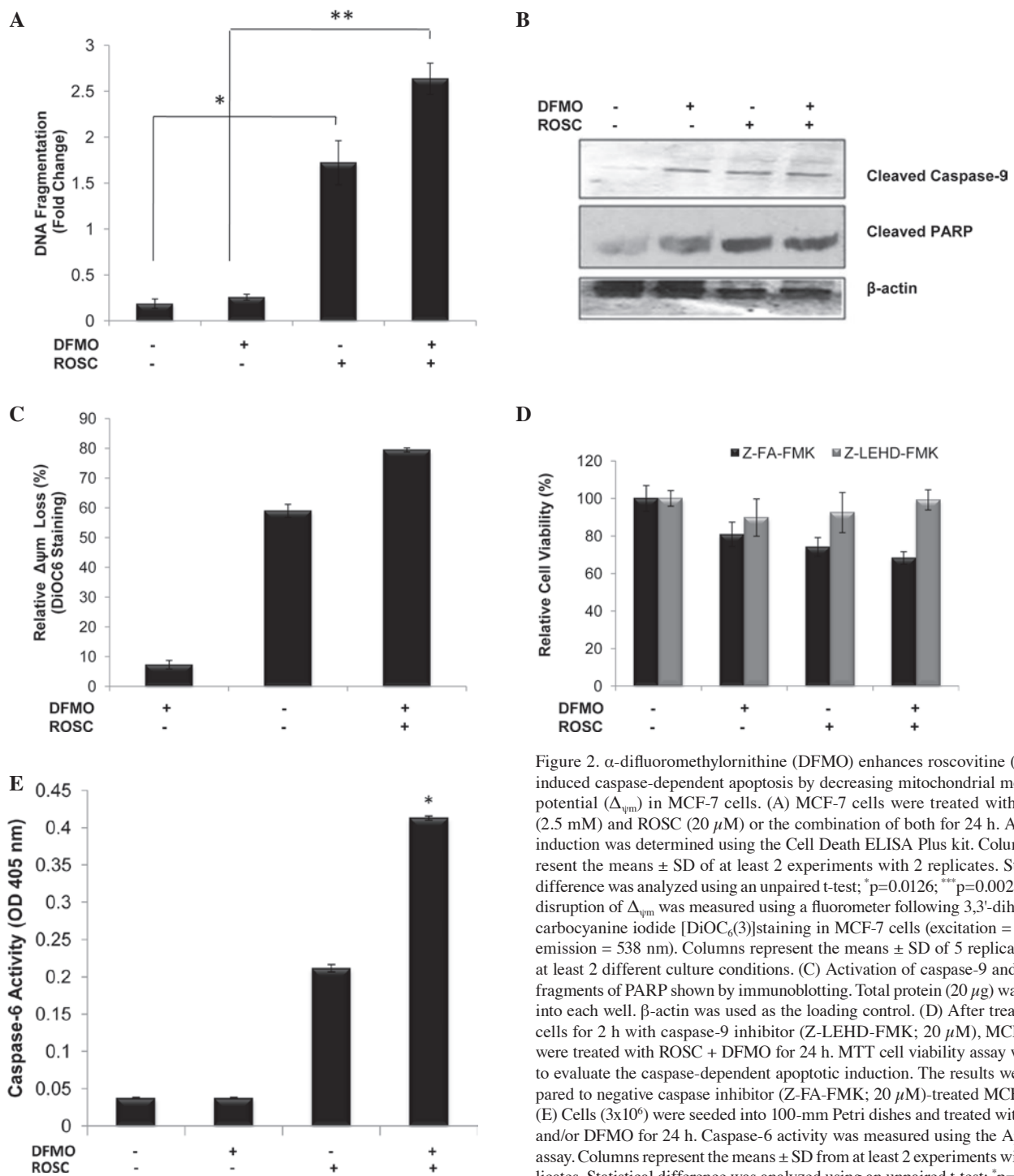
Figure 2. α-difluoromethylornithine (DFMO) enhances roscovitine (ROSC)-induced caspase-dependent apoptosis by decreasing mitochondrial membrane potential ($\Delta_{\psi m}$) in MCF-7 cells. (A) MCF-7 cells were treated with DFMO (2.5 mM) and ROSC (20 μM) or the combination of both for 24 h. Apoptotic induction was determined using the Cell Death ELISA Plus kit. Columns represent the means ± SD of at least 2 experiments with 2 replicates. Statistical difference was analyzed using an unpaired t-test; *p=0.0126; ***p=0.002. (B) The disruption of $\Delta_{\psi m}$ was measured using a fluorometer following 3,3'-dihexyloxa-carbocyanine iodide [DiOC$_6$(3)]staining in MCF-7 cells (excitation = 485 nm, emission = 538 nm). Columns represent the means ± SD of 5 replicates from at least 2 different culture conditions. (C) Activation of caspase-9 and cleaved fragments of PARP shown by immunoblotting. Total protein (20 μg) was loaded into each well. β-actin was used as the loading control. (D) After treatment of cells for 2 h with caspase-9 inhibitor (Z-LEHD-FMK; 20 μM), MCF-7 cells were treated with ROSC + DFMO for 24 h. MTT cell viability assay was used to evaluate the caspase-dependent apoptotic induction. The results were compared to negative caspase inhibitor (Z-FA-FMK; 20 μM)-treated MCF-7 cells. (E) Cells (3x10^6) were seeded into 100-mm Petri dishes and treated with ROSC and/or DFMO for 24 h. Caspase-6 activity was measured using the ApoTarget assay. Columns represent the means ± SD from at least 2 experiments with 5 replicates. Statistical difference was analyzed using an unpaired t-test; *p=0.0141.

of caspase-9, caspase-6 activity was determined (Fig. 2E). PA depletion by treatment with DFMO enhanced the ROSC-induced caspase-6 activity in MCF-7 cells. ROSC and/or DFMO-induced apoptosis were also confirmed by the detection of PARP cleavage. DFMO increased the ROSC-induced PARP cleavage compared to the drug treatment-only samples (Fig. 2C). These results suggest that ROSC is a strong apoptotic inducer agent which, by activating caspases and the depletion of PAs by DFMO treatment, increases ROSC-induced apoptosis.

Specific inhibition of ODC by DFMO increases ROSC-induced reactive oxygen species generation. In order to understand the

consequent events by the alteration of $\Delta_{\psi m}$, the generation of reactive oxygen species was found critical in mitochondrial-mediated apoptosis. We determined that ROSC induced the generation of reactive oxygen species. PA depletion enhanced the ROSC-induced apoptosis by increasing the levels of reactive oxygen species (Fig. 3A). To investigate the potential role of reactive oxygen species in ROSC-induced apoptosis, we also tested the protective effects of anti-oxidants. Cells were co-treated with various anti-oxidants, such as Trolox, α-tocopherol, N-acetyl-cysteine (NAC) and Put, with ROSC for 24 h. As shown in Fig. 3B, Trolox and α-tocopherol, which inhibits lipid peroxidation of cellular membranes, prevented

A

B
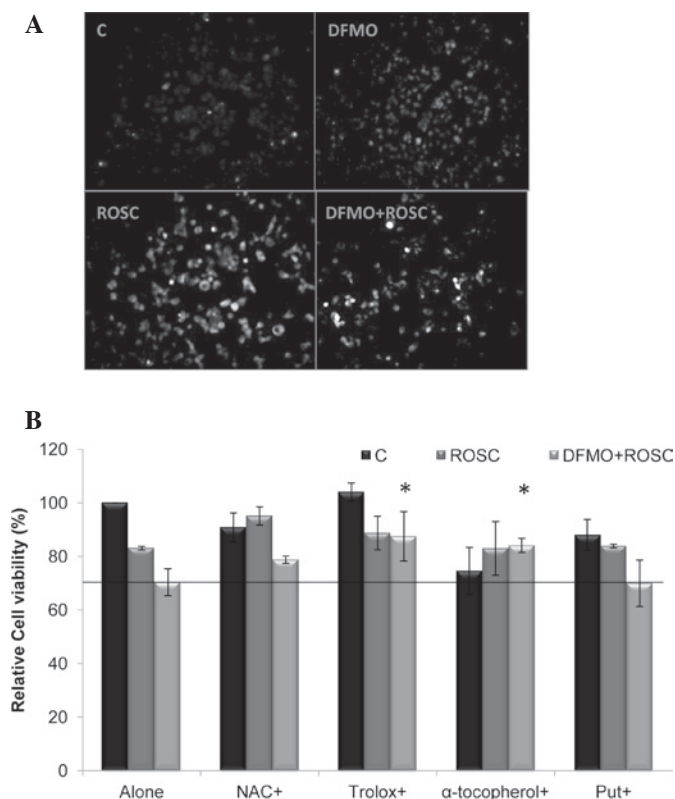
Figure 3. The generation of reactive oxygen species was increased following ROSC treatment in the presence or absence of DFMO. (A) Cells (1x10⁴) were seeded into a 96-well plate and treated with ROSC and/or DFMO for 24 h. Following DCFH-DA staining for 30 min, cells were visualized with fluorescence microscopy (excitation = 485 nm, emission = 538 nm). Columns represent the means ± SD of at least 2 experiments with 4 replicates. Statistical difference was analyzed using an unpaired t-test. (B) MCF-7 cells co-treated with DFMO, ROSC and various antioxidants; 5 μM NAC, 50 μM Trolox, 25 μM α-tocopherol and 10 μM Put. MTT cell viability was performed to determine the cell viability. Statistical difference was analyzed using an unpaired t-test; *p<0.05. C, control, untreated cells; DFMO, α-difluoromethylornithine; ROSC, roscovitine; DCFH-DA, 2',7'-dichlorofluorescein diacetate; NAC, N-acetyl-cysteine; Put, putrescine.

DFMO + ROSC-induced apoptosis (p<0.05). Although the co-treatment with the hydrogen superoxide scavenger, NAC, prevented ROSC-induced reactive oxygen species generation, it did not exert the same effect in the presence of DFMO. Put had a similar effect. Put co-treatment with ROSC in the presence or absence of DFMO did not prevent the cell viability loss.

Modulation of Bcl-2 family members. We investigated the modulation of Bcl-2 family members in ROSC-induced apoptosis in the presence or absence of ODC inhibitor to determine the involvement of the mitochondrial pathway-activated apoptotic mechanism. Therefore, we performed an immunoblot assay for the detection of the anti-apoptotic proteins, Bcl-2 and Bcl-x$_L$, and the pro-apoptotic proteinsm Puma, Bax, Bak and Bad. Exposure of the cells to ROSC did not alter Bcl-2 expression, but significantly downregulated anti-apoptotic Bcl-x$_L$. ROSC treatment led to the modulation of pro-apoptotic Bcl-2 family proteins; Puma α, Bax and Bad were upregulated in both ROSC and/or DFMO-treated samples compared to the control MCF-7 cells (Fig. 4).

A
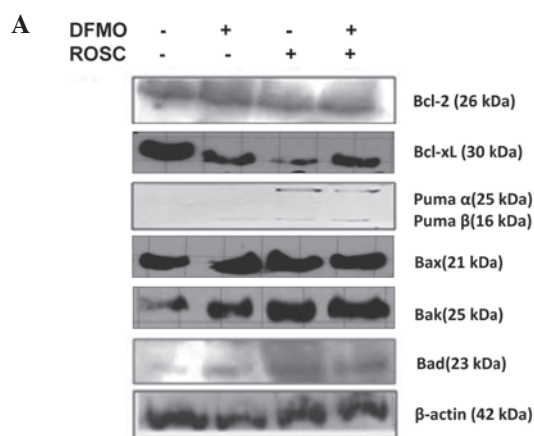
B

Western blot band intensities relative to β-actin						
	Bcl-2	Bcl-x$_L$	Puma α	Puma β	Bax	Bak	Bad
Control	0,66	1,65	0,62	0,61	0,90	0,70	0,18
DFMO	0,81	1,16	0,66	0,67	1,07	0,88	0,42
ROSC	0,65	1,21	0,75	0,84	1,13	1,01	0,81
DFMO+ROSC	0,68	1,41	0,78	0,80	1,11	1,12	0,78

Figure 4. Modulation of Bcl-2 family members following ROSC treatment in the presence or absence of DFMO was determined by immunoblotting method. (A) A total 30 μg of whole cell lysate was loaded in 10% sodium dodecyl sulphate-polyacrylamide gels and probed with Bcl-2 and Bcl-x$_L$ (anti-apoptotic proteins), and Puma, Bax, Bak and Bad (pro-apoptotic proteins). β-actin was used as the loading control. (B) Intensities relative to the β-actin control were measured by ImageJ software. DFMO, α-difluoromethylornithine; ROSC, roscovitine.
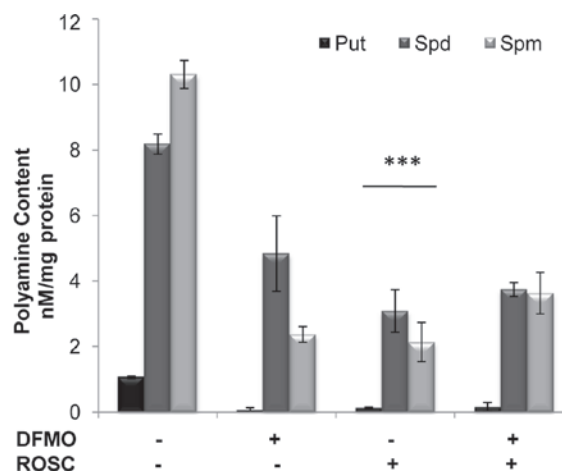
Figure 5. ROSC decreased intracellular PA contents in MCF-7 cells. Cells (3x10⁵) were seeded into 6-well plates. Cells were treated with ROSC in the presence or absence of DFMO. PA content was determined by the benzoylation method. Columns represent the means ± SD from 2 experiments with at least 2 replicates. Put, putrescine; Spd, spermidine; Spm, spermine; DFMO, α-difluoromethylornithine; ROSC, roscovitine. Statistical difference was analyzed using an unpaired t-test; ***p<0.0005.

ROSC alters intracellular PA levels. To investigate the potential role of PAs in ROSC-induced apoptosis in MCF-7 cells,

we determined the alteration of total PA levels. DFMO, ROSC or the combined treatment of both significantly decreased the content of Put, Spd and Spm, respectively (Fig. 5; p<0.005 vs. control). Although co-treatment of cells with DFMO and ROSC significantly decreased PA levels (p<0.0001) compared to the control samples, we did not obtain any significant changes compared to the drug treatment-only cases.

Discussion

Despite the presence of highly specific therapeutic options to obtain better results presenting long-term disease-free conditions, the metastatic breast cancer mortality rate remains high. Therefore, the identification of a molecular basis of new therapeutic targets, such as CDK inhibitors causing cell-cycle arrest, is gaining importance. The purine derivative, ROSC, is one of the most promising CDK inhibitors and provides a useful therapeutic strategy in breast cancer prevention and therapy (18). The antitumor action of ROSC has been demonstrated in a variety of cancer cell lines, including colon, prostate, leukemia and breast cancers (19). It has been shown that ROSC efficiently inhibits the proliferation of exponentially growing human MCF-7 cells (6).

The metabolic regulation of PAs has therapeutic potential, since PAs have been shown to play a crucial role in malignant cell proliferation and progression of disease. Therefore, the PA biosynthetic enzyme, ODC, has been highlighted as a therapeutic target for cancer prevention. The depletion of PAs by treatment with the ODC inhibitor, DFMO, has been shown to result in growth inhibition and lead to a significant increase in apoptosis (20). Furthermore, *in vivo* and *in vitro* studies have revealed that DFMO has an antiproliferative effect in various types of breast cancer cells (21).

In the present study, we demonstrate that a moderate cytotoxic concentration of ROSC (20 μM) decreases cell viability in a dose-dependent manner. Similar to our previous findings (22) obtained from HCT116 colon carcinoma cells, DFMO treatment (2.5 mM) increased the cell viability loss following ROSC treatment in MCF-7 cells (Fig. 1). We also determined that ROSC significantly induced apoptosis by decreasing $\Delta_{\psi m}$, and DFMO increased the ROSC-induced apoptosis in metastatic MCF-7 breast cancer cells (Fig. 2). Therefore, we can conclude that ROSC is a successful apoptotic inducer and that the modulation of intracellular PAs may be critical in the ROSC-induced apoptosis in MCF-7 cells. In accordance with our findings, ROSC has been shown to be a successful apoptotic inducer in MCF-7 and MDA-MB-231 breast cancer cells (23,24). It has also been reported that overexpression of antizyme, which functions as an ODC inhibitor, augments doxorubicin-induced apoptosis independently of the cell cycle in human leukemia HL-60 cells, acute T leukemia Jurkat cells and mouse macrophage RAW 264.7 cells (25). The results of the present study suggest the significance of targeting ODC as a potential therapeutic target to promote the drug-induced apoptosis.

As shown in previous studies, ROSC-induced apoptotic cell death has been found to be caspase-dependent in MCF-7 cells (26). Although MCF-7 cells were caspase-3 null, DFMO showed additive effects in ROSC-induced caspase-9 activation. Prior treatment with caspase inhibitors followed by ROSC treatment prevented apoptotic induction in MCF-7 cells.

Similar to previous reports, we found that the generation of reactive oxygen species upon ROSC treatment correlated with PA metabolism in MCF-7 cells (27). The PA catabolic pathway, which is represented by the activity of the key enzymes, spermidine/spermine N1-acetyltransferase (SSAT), N1-polyamine oxidase (PAO) or spermine oxidase (SMO/PAOh1), may be upregulated by the treatment of various chemotherapeutic agents. The elevated enzyme activity leads to significant decrease in PA content and induced generation of byproducts, such as hydrogen peroxide, which is a strong apoptotic inducer (28). Therefore, we determined the cell viability following drug treatment in the presence of anti-oxidant scavengers. As shown in Fig. 3, the inhibition of drug-modulated lipid peroxidation by Trolox or α-tocopherol treatment significantly prevented cell viability decrease following drug treatment in MCF-7 cells. Although NAC was a successful hydrogen peroxide scavenger, it did not prevent drug-induced cytotoxic effects in MCF-7 cells. Put treatment had similar effects. Notably, when ODC was inhibited by DFMO, co-treatment with Put enhanced the ROSC-induced cell viability loss (Fig. 3B), and this effect was found to be irreversible. Taken together, these results reveal that PA catabolic metabolism may play a role in ROSC-induced apoptosis. Therefore, further studies are required to investigate the possible role of PAs in ROSC-induced apoptosis with the involvement of the PA catabolic enzymes.

Since Bcl-2 family members have been shown to be critical regulators of apoptotic cell death, we investigated the modulation of several pro- and anti-apoptotic Bcl-2 family members to determine the involvement of ROSC-induced apoptosis (29,30). We found that ROSC was more effective in the downregulation of Bcl-x$_L$ than Bcl-2, which are known as genes responsible for drug resistance (Fig. 4). Pro-apoptotic Puma α and β, Bax and Bad were found to be upregulated following treatment with ROSC alone (Fig. 4). Previous findings have indicated that ROSC treatment diminishes the cyclin A1 levels and increases Cdk2 inhibition (31). Cdk2 catalyzes Bad phosphorylation at serine-128, which in turn decreases the mitochondrial threshold for apoptosis (32). Therefore, we conclude that Bad upregulation may be critical in ROSC-induced apoptosis in MCF-7 cells.

Previous reports have suggested that the elevated cellular PA content may induce breast cancer progression and this has been linked to the aggressive phenotype of breast tumors (28). In this study, we showed that, similar to DFMO, ROSC altered intracellular PA content (Fig. 5). However DFMO treatment did not exert any additive effect in alteration of PA levels following ROSC treatment in MCF-7 cells. Therefore, further research is required to put forward the mechanistic role of ROSC in PA metabolism.

In conclusion, as a novel CDK inhibitor, ROSC activates mitochondrial-mediated apoptosis in estrogen-dependent MCF-7 cancer cells caspase-dependently. Our results show that the apoptotic induction concurrently led to a significant increase in reactive oxygen species, and this effect was found to be reversible by co-treatment with lipid peroxidation inhibitors. The specific inhibition of the PA biosynthetic enzyme, ODC, by DFMO treatment altered ROSC-induced apoptotic events by altering intracellular PA content. All these findings may be critical in clarifying the regulatory role of the PA metabolic pathway in drug-induced apoptosis. Our study also

confirms that ROSC as a CDK inhibitor is a potential therapeutic target in estrogen-dependent breast cancer cells.

Acknowledgements

References

1. Jemal A, Siegel R, Ward E, Hao Y, Xu J and Thun MJ: Cancer statistics, 2009. CA Cancer J Clin 59: 225-249, 2009.
2. Ma H, Bernstein L, Ross RK and Ursin G: Hormone-related risk factors for breast cancer in women under age 50 years by estrogen and progesterone receptor status: results from a case-control and a case-case comparison. Breast Cancer Res 8: R39, 2006.
3. Al-Minawi AZ, Saleh-Gohari N and Helleday T: The ERCC1/XPF endonuclease is required for efficient single-strand annealing and gene conversion in mammalian cells. Nucleic Acids Res 36: 1-9, 2008.
4. Hunt T: You never know: Cdk inhibitors as anti-cancer drugs. Cell Cycle 7: 3789-3790, 2008.
5. Aldoss IT, Tashi T and Ganti AK: Seliciclib in malignancies. Expert Opin Investig Drugs 18: 1957-1965, 2009.
6. Maurer M, Komina O and Wesierska-Gadek J: Roscovitine differentially affects asynchronously growing and synchronized human MCF-7 breast cancer cells. Ann NY Acad Sci 1171: 250-256, 2009.
7. Hoggard N and Green CD: Polyamines and growth regulation of cultured human breast cancer cells by 17 beta-oestradiol. Mol Cell Endocrinol 46: 71-78, 1986.
8. Manni A: Polyamine involvement in breast cancer phenotype. In Vivo 16: 493-500, 2002.
9. Manni A, Wechter R, Grove R, Wei L, Martel J and Demers L: Polyamine profiles and growth properties of ornithine decarboxylase overexpressing MCF-7 breast cancer cells in culture. Breast Cancer Res Treat 34: 45-53, 1995.
10. Manni A, Astrow SH, Gammon S, Thompson J, Mauger D and Washington S: Immunohistochemical detection of ornithine-decarboxylase in primary and metastatic human breast cancer specimens. Breast Cancer Res Treat 67: 147-156, 2001.
11. Manni A, Grove R, Kunselman S and Aldaz CM: Involvement of the polyamine pathway in breast cancer progression. Cancer Lett 92: 49-57, 1995.
12. Jun JY, Griffith JW, Bruggeman R, et al: Effects of polyamine depletion by alpha-difluoromethylornithine on in vitro and in vivo biological properties of 4T1 murine mammary cancer cells. Breast Cancer Res Treat 105: 29-36, 2007.
13. Richert MM, Phadke PA, Matters G, et al: Metastasis of hormone-independent breast cancer to lung and bone is decreased by alpha-difluoromethylornithine treatment. Breast Cancer Res 7: R819-R827, 2005.
14. Simoneau AR, Gerner EW, Nagle R, et al: The effect of difluoromethylornithine on decreasing prostate size and polyamines in men: results of a year-long phase IIb randomized placebo-controlled chemoprevention trial. Cancer Epidemiol Biomarkers Prev 17: 292-299, 2008.
15. Sporn MB and Hong WK: Concomitant DFMO and sulindac chemoprevention of colorectal adenomas: a major clinical advance. Nat Clin Pract Oncol 5: 628-629, 2008.
16. Rounbehler RJ, Li W, Hall MA, Yang C, Fallahi M and Cleveland JL: Targeting ornithine decarboxylase impairs development of MYCN-amplified neuroblastoma. Cancer Res 69: 547-553, 2009.
17. Singh AB, Thomas TJ, Thomas T, Singh M and Mann RA: Differential effects of polyamine homologues on the prevention of DL-alpha-difluoromethylornithine-mediated inhibition of malignant cell growth and normal immune response. Cancer Res 52: 1840-1847, 1992.
18. Senderowicz AM: Cyclin-dependent kinases as new targets for the prevention and treatment of cancer. Hematol Oncol Clin North Am 16: 1229-1253, 2002.
19. Edamatsu H, Gau CL, Nemoto T, Guo L and Tamanoi F: Cdk inhibitors, roscovitine and olomoucine, synergize with farnesyltransferase inhibitor (FTI) to induce efficient apoptosis of human cancer cell lines. Oncogene 19: 3059-3068, 2000.
20. Davidson NE, Hahm HA, McCloskey DE, Woster PM and Casero RA Jr: Clinical aspects of cell death in breast cancer: the polyamine pathway as a new target for treatment. Endocr Relat Cancer 6: 69-73, 1999.
21. Meyskens FL Jr and Gerner EW: Development of difluoromethylornithine (DFMO) as a chemoprevention agent. Clin Cancer Res 5: 945-951, 1999.
22. Arisan ED, Coker A and Palavan-Unsal N: Polyamine depletion enhances the roscovitine-induced apoptosis through the activation of mitochondria in HCT116 colon carcinoma cells. Amino Acids: Aug 2, 2011 (Epub ahead of print).
23. Wojciechowski J, Horky M, Gueorguieva M and Wesierska-Gadek J: Rapid onset of nucleolar disintegration preceding cell cycle arrest in roscovitine-induced apoptosis of human MCF-7 breast cancer cells. Int J Cancer 106: 486-495, 2003.
24. Mgbonyebi OP, Russo J and Russo IH: Roscovitine induces cell death and morphological changes indicative of apoptosis in MDA-MB-231 breast cancer cells. Cancer Res 59: 1903-1910, 1999.
25. Liu GY, Liao YF, Hsu PC, et al: Antizyme, a natural ornithine decarboxylase inhibitor, induces apoptosis of haematopoietic cells through mitochondrial membrane depolarization and caspases' cascade. Apoptosis 11: 1773-1788, 2006.
26. Wesierska-Gadek J, Gueorguieva M and Horky M: Dual action of cyclin-dependent kinase inhibitors: induction of cell cycle arrest and apoptosis. A comparison of the effects exerted by roscovitine and cisplatin. Pol J Pharmacol 55: 895-902, 2003.
27. Macip S, Igarashi M, Fang L, et al: Inhibition of p21-mediated ROS accumulation can rescue p21-induced senescence. EMBO J 21: 2180-2188, 2002.
28. Babbar N, Murray-Stewart T and Casero RA Jr: Inflammation and polyamine catabolism: the good, the bad and the ugly. Biochem Soc Trans 35: 300-304, 2007.
29. Arisan ED, Kutuk O, Tezil T, Bodur C, Telci D and Basaga H: Small inhibitor of Bcl-2, HA14-1, selectively enhanced the apoptotic effect of cisplatin by modulating Bcl-2 family members in MDA-MB-231 breast cancer cells. Breast Cancer Res Treat 119: 271-281, 2010.
30. Leung LK and Wang TT: Differential effects of chemotherapeutic agents on the Bcl-2/Bax apoptosis pathway in human breast cancer cell line MCF-7. Breast Cancer Res Treat 55: 73-83, 1999.
31. Federico M, Symonds CE, Bagella L, et al: R-Roscovitine (Seliciclib) prevents DNA damage-induced cyclin A1 upregulation and hinders non-homologous end-joining (NHEJ) DNA repair. Mol Cancer 9: 208, 2010.
32. Hashimoto A, Hirose K and Iino M: BAD detects coincidence of G2/M phase and growth factor deprivation to regulate apoptosis. J Biol Chem 280: 26225-26232, 2005.